An accelerated boundary element method using fast Fourier transform on multipoles

Kian-Meng Lim[a,*], Eng-Teo Ong[b], Heow-Pueh Lee[a,b]

[a] *Mechanical Engineering, National University of Singapore, Singapore 117576*
[b] *Institute of High Performance Computing, Singapore 117528*

Abstract

We present a fast algorithm, called the fast Fourier transform on multipoles (FFTM) method, for accelerating the boundary element method. The algorithm employs the multipole and local expansions to approximate far-field potentials and exploits the discrete convolution nature of the multipole to local translation operator to accelerate the potential evaluation process. The method is illustrated with a three-dimensional acoustics scattering problem governed by the Helmholtz equation. It is shown that the method has approximately linear computational complexity and it achieves accurate results with a relatively low order of expansion.

Keywords: Boundary element method; Multipole; Fast Fourier transform; Acoustics scattering

1. Introduction

The boundary element method (BEM) is an effective numerical method for solving acoustics problems governed by the Helmholtz equation. It is particularly suitable for infinite domain problems, since no artificial truncation of domain and specification of boundary conditions at infinity are required. However, the conventional BEM generates a dense linear system, which requires $O(N^3)$ and $O(N^2)$ operations when solved using Gaussian elimination and iterative methods (such as generalized minimal residuals (GMRES), respectively, where N is the number of unknowns in the problem. The computational requirements become prohibitively large when the problem size N increases to hundreds of thousands.

To improve the computation speed, numerous fast algorithms have been developed. The fast multipole method (FMM) is one of the most widely implemented algorithms [1–4]. Another group of fast methods utilizes the fast Fourier transform (FFT) to accelerate the matrix–vector product operation. They include the particle-mesh-based approach [5], the precorrected FFT method [6], and a variant of the latter [7].

In this paper, we present an alternative fast algorithm based on an important observation that the multipole-to-local expansions translation operator in the potential evaluation process can be expressed as a series of discrete convolutions of the multipole moments with their associated spherical harmonics functions. FFT algorithms can be employed to evaluate these discrete convolutions rapidly. We refer to this new algorithm as the fast Fourier transform on multipoles (FFTM) method. This algorithm has been applied to solve the Laplace equation in electrostatic analysis [8]. Here, we will demonstrate this method for solving the Helmholtz equation.

2. Formulation

We consider the Helmholtz equation for a complex potential $\psi(\boldsymbol{x})$ given by

$$\nabla^2 \psi(\boldsymbol{x}) + k^2 \psi = 0, \quad \mathbf{x} \in \Omega \tag{1}$$

where k is the wavenumber. The domain of interest Ω is unbounded and the solution has to satisfy the Sommerfeld radiation condition

$$\lim_{r\to\infty} r\left(\frac{\partial \psi}{\partial r} - ik\psi\right) = 0, \qquad r = \|\boldsymbol{r}\| \tag{2}$$

where $\|\cdot\|$ denotes the Euclidean norm and $\mathrm{i} = \sqrt{-1}$.

* Corresponding author. Tel.: +65 6874 8860; Fax: +65 6779 1459; E-mail: limkm@nus.edu.sg

Computational Fluid and Solid Mechanics 2005
K.J. Bathe (Editor)

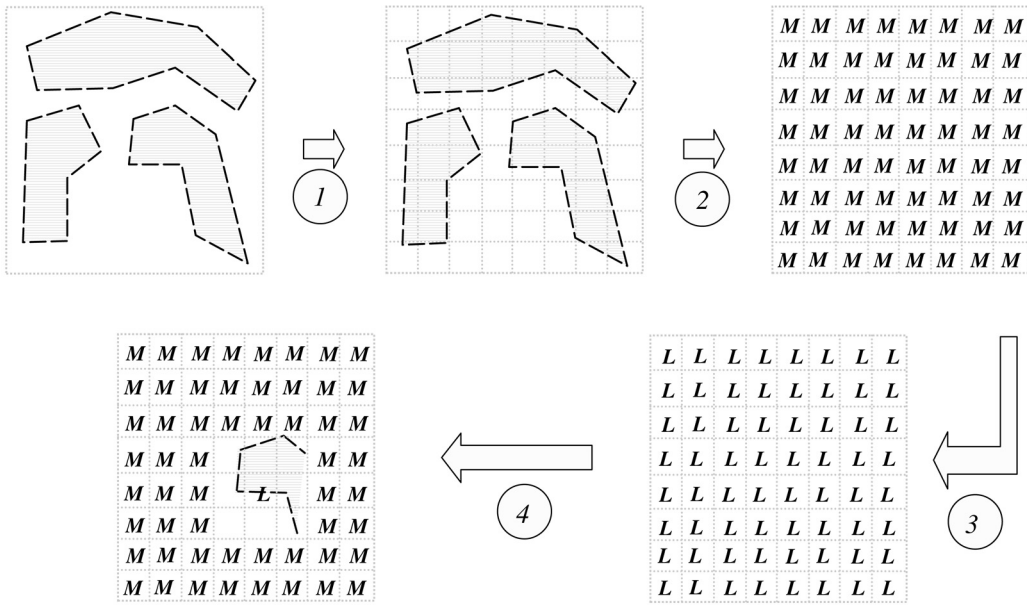

Fig. 1. Two-dimensional pictorial representation of the FFTM algorithm. Step 1: division of problem domain into many smaller cells and allocation of elements. Step 2: computation of multipole moments M for all cells. Step 3: evaluation of local expansion coefficients L at cell centers by discrete convolutions via FFT. Step 4: for each cell, computation of potentials at nodal locations using L, which accounts for effects from 'distant' elements, and addition of the 'near' source contributions directly.

The boundary integral equation for this problem is given by

$$\alpha(\mathbf{x})\psi(\mathbf{x}) = \int_{\Gamma} \left[\frac{\partial \psi(\mathbf{x}')}{\partial n} G(\mathbf{x},\mathbf{x}') - \psi(\mathbf{x}') \frac{\partial G(\mathbf{x},\mathbf{x}')}{\partial n} \right] d\Gamma(\mathbf{x}') \tag{3}$$

where $\boldsymbol{x}$ and $\boldsymbol{x}'$ denote the field and source points, respectively, and $\alpha(\boldsymbol{x})$ is generally known as the jump term, which arises when $\boldsymbol{x}$ is moved to the boundary and is dependent on the geometry of the boundary at $\boldsymbol{x}$. The fundamental solution $G(\boldsymbol{x},\boldsymbol{x}')$ is given by

$$G(\mathbf{x},\mathbf{x}') = \frac{e^{ik|\mathbf{x}-\mathbf{x}'|}}{4\pi\|\mathbf{x}-\mathbf{x}'\|} \tag{4}$$

for the three-dimensional case.

The boundary element method divides the boundary Γ into small elements and approximates the field variables in terms of nodal variables to give a dense linear system of equations.

$$\mathbf{A}\vec{X} = \vec{B} \tag{5}$$

where $\boldsymbol{A}$ is a fully populated $N \times N$ coefficient matrix and $\vec{X}$ and $\vec{B}$ are $N \times 1$ column vectors with $\vec{X}$ containing the unknown variables. The system of equations is solved using iterative methods (such as GMRES), and the FFTM algorithm is applied in the inner loop to speed up the matrix–vector multiplication by providing a sparse representation of $\boldsymbol{A}$. This consists of four steps, as illustrated in Fig. 1.

2.1. Step 1: spatial discretization

This step divides a rectangular volume that contains all the elements into many smaller cells and allocates the elements among the cells. The aim is to identify closely packed elements that can be approximated by multipole moments and to separate the 'near' neighboring elements and the 'distant' elements.

2.2. Step 2: conversion of clusters of elements into multipole moments

The operator, denoted by ***Q2M***, converts a cluster of n_q elements in a cell to an equivalent set of multipoles at the centre of the cell:

$$M_n^m = \sum_{i=1}^{n_q} \int_{\Gamma_e} f(\rho_i,\alpha_i,\beta_i) j_n(k\rho_i) Y_n^{-m}(\alpha_i,\beta_i) d\Gamma \tag{6}$$

where $f(\rho,\alpha,\beta)$ is the source distribution on each element, $j_n(kr)$ is the Bessel function of the first kind that

satisfies the Sommerfeld condition, and $Y_n^{-m}(\theta,\phi)$ is the spherical harmonic of degree n and order m.

2.3. Step 3: evaluation of local expansion coefficients due to multipole moments

An intermediate set of local expansion coefficients are obtained at the center of all cells by

$$L_s^t = \sum_{n=0}^{\infty} \sum_{m=-n}^{a} T_{s,n}^{t,m} M_n^m \tag{7}$$

where $T_{s,n}^{t,m}$ is the transfer function given by

$$T_{s,n}^{t,m} = \sum_{a=0}^{\infty} \sum_{b=-a}^{a} \upsilon_{ans}^{bmt} h_a(kr)\, Y_a^b(\theta,\phi) \tag{8}$$

where υ_{ans}^{bmt} is a coefficient related to the Wigner 3-j symbols, and a set of recurrence formulae have been derived to evaluate them efficiently [9].

The translation formula for multipole expansions (truncated to order p) to local expansions for the entire grid can be written as a series of three-dimensional discrete convolutions:

$$L_s^t(x,y,z) \approx \sum_{n=0}^{p} \sum_{m=-n}^{n} \left[\sum_{x'} \sum_{y'} \sum_{z'} T_{s,n}^{t,m}(x-x', y-y', z-z') M_n^m(x',y',z') \right] \tag{9}$$

where the indices (x, y, z), and (x',y',z') denote the discrete cell center locations of the field points and multipole moments. Due to the regular spacing of the cell centers, the local expansion coefficients can be evaluated rapidly all at once using FFT algorithms. To evaluate the potential in a given cell, the effect of the multipole moments from its neighbors are often inaccurate. We overcome this problem by performing a local correction, which involves (i) removing the inaccurate contributions from the 'near' multipole moments by setting

$$T_{s,n}^{t,m}(x-x', y-y', z-z') = 0, \quad \text{for } |x-x'|,\ |y-y'| \text{ and } |z-z'| \le D \tag{10}$$

where D corresponds to the layers of cells that are considered 'near', and (ii) replacing these erroneous results by those computed exactly as in the direct approach.

2.4. Step 4: evaluation of the potentials at nodal locations

The potentials at element nodal locations $\mathbf{y} = (r, \theta, \phi)$ due to 'distant' sources is computed using the ***L2P*** translation operator given by

$$\psi(y) = \sum_{s=0}^{p} \sum_{t=-s}^{s} L_s^t j_s(kr)\, Y_s^t(\theta,\phi) \tag{11}$$

The 'near' contributions are added directly to the nodal locations, denoted by ***Q2P***.

The computation time and memory storage needed for 'cell-centered' operations, ***Q2M***, ***L2P***, and ***Q2P*** scales linearly with N. For FFT operations, the storage and time needed are $O(N_c)$ and $O(N_c \log N_c)$, respectively, where N_c is the number of cells. Overall, the algorithm has near-linear complexity: $O(N)$, $O(N_c)$, and $O(N_c \log N_c)$ for large N and N_c.

3. Numerical example

In this example, we study the scattering pattern of a sound-hard cylinder submerged in water subjected to a

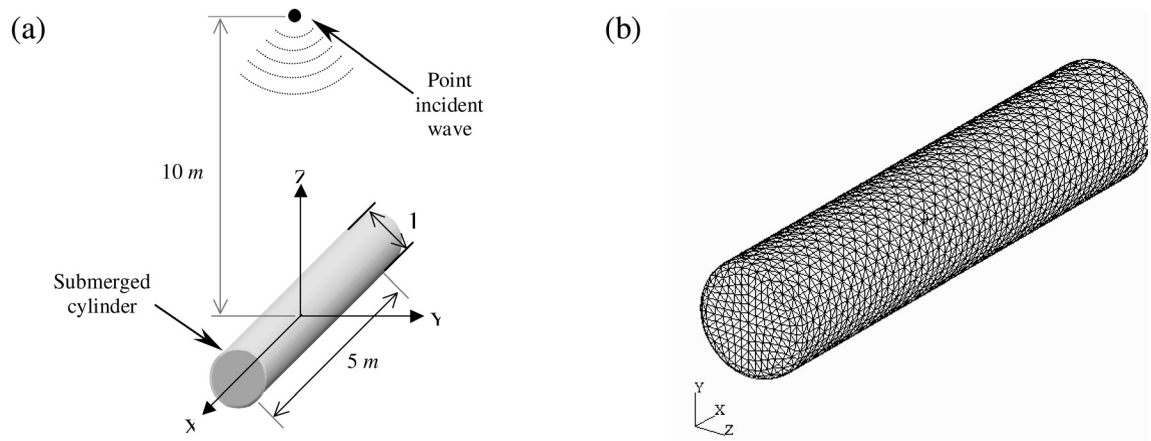

Fig. 2. (a) Schematic diagram for the scattering cylinder example in underwater acoustics analysis. (b) Element mesh of the cylinder with 2842 nodes and 5680 elements.

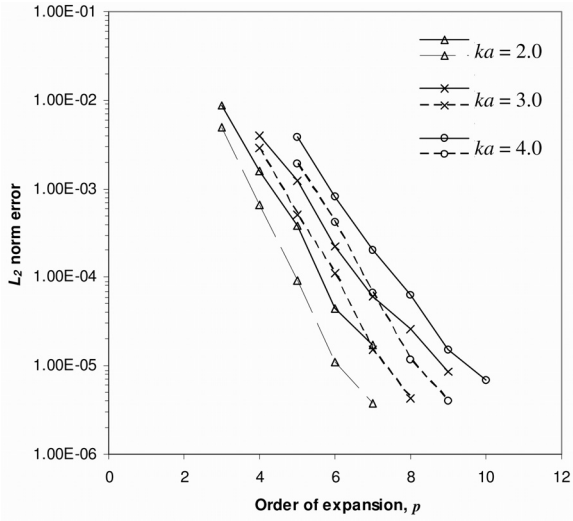

Fig. 3. L_2 norm error convergence plots for the surface pressure solutions using first-layer (solid lines) and second-layer (dashed lines) stencils for 'near' cells definition.

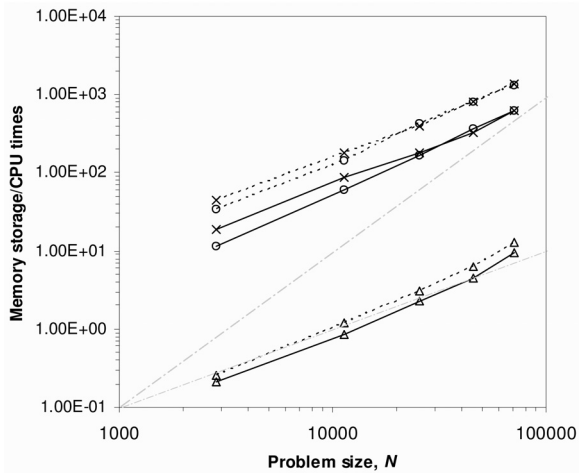

Fig. 4. Computational complexity plots of memory storage requirement in MB (x) and the CPU time in seconds at the intialization (◯) and iteration (Δ) stages, for $< 1.0\%$ (solid lines) and $< 0.1\%$ (dashed lines) accuracy.

point incident sound wave of unit magnitude at a frequency of 2 kHz. Fig. 2 shows the schematic diagram and the element mesh of the problem.

To study the accuracy of the method, we obtain the error in the L_2 norm for the pressure distribution as given by

$$Error = \left(\frac{\sum_{i=1}^{N} \left| P_i^{BEM} - P_i^{FFTM} \right|^2}{\sum_{i=1}^{N} \left| P_i^{BEM} \right|^2} \right)^{\frac{1}{2}} \tag{12}$$

where P_i^{BEM} and P_i^{FFTM} are ith nodal surface pressure of the standard BEM and the FFTM schemes, respectively. The analysis was done using the first- ($M = 27$) and second- ($M = 125$) layer stencils for the 'near' cells, and the error plots are depicted in Fig. 3.

The FFTM was found to give accurate solutions using a relatively low order of expansion. From the plots, it is observed that the FFTM schemes can achieve an error of less than 1.0% if $p \geq (ka + 2)$ and an error of less than 0.1% if $p \geq (ka + 3)$. In general, the second-layer stencil schemes tend to give more accurate results and have slightly faster convergence rates.

The computation using FFTM is then repeated for five different incident wave frequencies, ranging from 2 to 10 kHz at an interval of 2 kHz. The corresponding problem sizes are 2842, 11 362, 25 562, 45 442, and 71 002, respectively, as smaller elements are required to capture the rapidly oscillating field at a higher frequency. The computational complexity in terms of memory storage and CPU time is depicted in Fig. 4. From the plots, we observe that the curves can be approximated by power functions of the form AN^B, with B ranging from 1.05 to 1.07 for the memory storage requirement and from 1.14 to 1.24 for the CPU time. The deviation from linear growth in complexity is probably due to the presence of $O(N \log N)$ complexity in the FFT operations.

4. Conclusion

An FFTM algorithm has been developed for efficient solution of the Helmholtz equation. It is demonstrated that the algorithm can achieve reasonably good accuracy with a relatively low order of expansion. This algorithm is also simple to implement compared with the more complicated hierarchical structure in the FMM.

References

[1] Greengard L, Rokhlin V. A fast algorithm for particle simulations. J Comput Phys 1987;73:325–348.
[2] Nabors K, White J. Fastcap: a multipole accelerated 3-D capacitance extraction program. IEEE Trans CAD Integr Circuits Systems 1991;11:1447–1459.
[3] Song JM, Lu CC, Chew WC, Lee SW. Fast Illinois Solver Code (FISC). IEEE Antennas Propag 1998;40:27–34.
[4] Darve E. The fast multipole method: numerical implementation. J Comput Phys 2000;160:195–240.
[5] Luty BA, van Gunsteren WF. Calculating electrostatic interactions using particle-particle-particle-mesh method with nonperiodid long-range interactions. J Chem Phys 1996;100:2581–2587.

[6] Phillips JR, White J. A precorrected-FFT method for electrostatic analysis of complicated 3-D structures. IEEE Trans CAD Integr Circuits Systems 1997;16:1059–1072.
[7] Bruno OP, Kunyansky LA. A fast, high-order algorithm for the solution of surface scattering problems: basic implementation, tests and applications. J Comput Phys 2001;169:80–110.
[8] Ong ET, Lee HP, Lim KM. A parallel fast Fourier transform on multipoles (FFTM) algorithm for electrostatics analysis of three-dimensional structures. IEEE Trans CAD Integr Circuits Systems 2004;23:1063–1072.
[9] Gumerov NA, Duraiswami R. Fast, exact, and stable computation of multipole translation and rotation coefficients for the 3D Helmholtz equation. Technical report UMIACS-TR#2001–44, University of Maryland Instititute for Advanced Computer Studies, 2001.